Topological optimization of nonlinear optical quantum wire networks

Rick Lytel, Shoresh Shafei, and Mark G. Kuzyk

Department of Physics and Astronomy, Washington State University, Pullman, Washington 99164-2814

ABSTRACT

Spatially extended molecular structures, modeled as quantum graphs with one-dimensional electron dynamics, exhibit optical responses that can approach the fundamental limits. We present the results of a comprehensive study of the topological dependence of the nonlinearities of quantum graphs and show exactly how the first and second hyperpolarizability of a graph depend upon its topological class and how the hyperpolarizability tensors vary with graph geometry. We show how graphs with star motifs share universal scaling behavior near the maximum nonlinear responses and articulate design rules for quantum-confined, quasi-one dimensional systems that may be realized using molecular elements and nanowires.

Keywords: quantum graphs, hyperpolarizability, fundamental limit, quantum confined systems, quantum wire, nonlinear optical quantum graphs

1. INTRODUCTION

The optimization of molecular structures to achieve large, intrinsic first and second hyperpolarizabilities is a prelude to assembling highly active materials for applications in nonlinear optics. In 2012, we launched the first comprehensive study of the nonlinear optical properties of quantum graphs in order to determine how electron confinement to one dimension and variation in geometry of a variety of topological structures might enhance the nonlinear optical response.[1–4] Leveraging a one-dimensional model of a nonlinear optical quantum wire,[5] we developed a standard approach for Monte Carlo calculations of the hyperpolarizabilities of quantum graphs with arbitrary geometries for a given topology. We explored bent wire, closed and open loop, star, and more exotic topologies and discovered structures with nonlinearities approaching the fundamental limits. This paper summarizes our findings and discusses application to nanowires and assemblies.

Section 2 presents a concise summary of the analysis of nonlinear optical quantum graphs. Section 3 displays the main results of the study of the topological dependence of the nonlinearities and their control through geometry. Section 4 suggests physical systems that should be realizable. In the interest of brevity, each section relies heavily upon results and methods described in the literature. The reader is strongly encouraged to investigate the key references.

2. STANDARD MODEL OF NONLINEAR OPTICAL QUANTUM GRAPHS

A quantum graph is a network of metric edges connected at vertices, supporting particle dynamics with flux-conserving boundary conditions. The one-electron quantum graph is a well-studied, exactly solvable model of quantum chaos when motion is confined to the direction along the edges.[6–10] The electron on the graph is tightly bound in the transverse direction, yielding a quasi one-dimensional dynamical system. When coupled to optical fields, the quantum graph is a model of 1D nonlinear optical molecular structures exhibiting rich topological and geometrical properties.

email: rlytel@wsu.edu

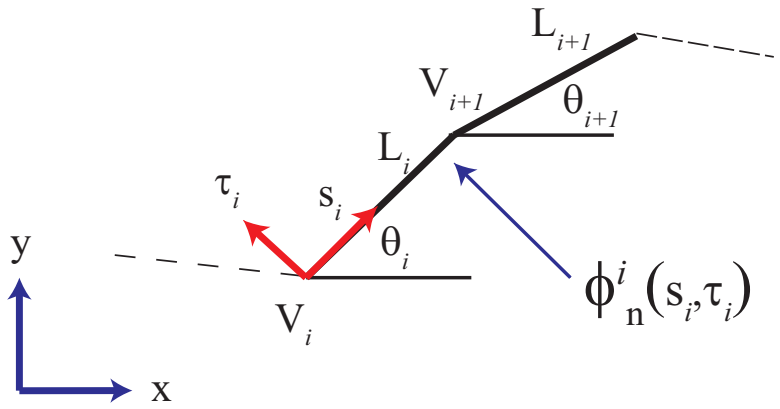

Figure 1. Quantum graph, showing the notation for the edges and vertices.

The dynamics of an electron on a single quantum wire in the limit of zero transverse dimension are described by a self-adjoint Hamiltonian with a complete set of eigenstates and energies.[11] The nonlinear optical hyperpolarizabilities of a single wire depend only on motion along the wire and are calculable using conventional sum over states methods.[1] The transition moments and energies satisfy the Thomas-Reiche-Kuhn (TRK) sum rules, which contain longitudinal sums as well as residual transverse contributions.[12]

Quantum graphs have several desirable properties for exploration as model nonlinear optical systems with potentially large hyperpolarizabilities. Their energy spectra are similar to those that maximize the hyperpolarizabilities in Monte Carlo studies of spectral effects on nonlinear response.[12] The confinement of particle motion to a single dimension models quantum confined systems for which larger nonlinear optical response is expected. Finally, the connections among the edges, and the sheer number of planar configurations of edges with respect to one another, provide an enormous space of possible shapes for a given topology, as well as a large number of topologies for study.

A typical quantum graph is shown in Fig 1, using the notation of our prior publications.[1–3] The transverse dimension τ is effectively removed from the one-dimensional problem via a limiting process.[5] The assembly of graphs from quantum wires is mathematically realized as a direct sum of Hilbert subspaces, one each for each wire, where the Hamiltonian is identical on each wire, as are the eigenvalues, but the edge functions differ. The full eigenstates of a graph such as that shown in Fig 1, are unions of the edge states:[1]

$$\psi_n(s) = \cup_{i=1}^{E} \phi_n^i(s_i) \tag{1}$$

The edge functions for an edge connecting a vertex with amplitude A_n to vertex with amplitude B_n may be written in a canonical form that automatically matches (nonzero) amplitudes at each internal vertex:

$$\phi_n^i(s_i) = \frac{A_n^{(i)} \sin k_n(a_i - s_i) + B_n^{(i)} \sin k_n s_i}{\sin k_n a_i} \tag{2}$$

At each vertex, the edge functions match in amplitude, and their derivatives sum to a net flux of zero into or out of a vertex. Terminated ends are modeled as infinite potentials, where edge functions vanish. The collection of boundary conditions, taken together, provide a set of simultaneous equations whose solution demands that the determinant of the coefficients vanishes. This produces a transcendental characteristic (secular) equation that provides the eigenvalues for the graph. The coefficients of the edge functions are then extracted and used to construct the eigenstates through the union operation. The eigenstates are then normalized, and the set of states and energies may be used to compute the nonlinear optical properties of the graph.

The transition moments for the graph are calculated using the full eigenstates and are sums over edges of the moments of the edge coordinate times an angular factor describing the geometric position of the edge relative to an external axis used to define the vertices of the graph:

$$x_{nm} = \sum_{i=1}^{E} \int_0^{a_i} \phi_n^{*i}(s_i)\phi_m^i(s_i)\ x(s_i)ds_i \tag{3}$$

where $\phi_m^i(s_i)$ are the normalized edge wave functions given in Eqn 2. Here, $x(s_i)$ is the x-component of s_i, measured from the origin of the graph (and not of the edge), and is a function of the prior edge lengths and angles. With edge wave functions of the form of Eqn (2), the computation of the transition moments requires integrals of products of sines and cosines with either s or 1, all of which are calculable in closed form. Detailed examples for loops, wires, and stars are available in the literature from our prior work.[1–3]

The vast space of configurations of quantum graphs is best simulated in a Monte Carlo calculation. In a typical simulation, a large set of random vertices is selected, and the connections among them are fixed and reflect the topology of the graph, such as a wire, loop or a star. The eigenvalues of the graphs satisfy the same characteristic equation that depends solely on the edge lengths, while the transition moments depend on the angular positions of the edges, as well as their lengths. For a fixed topology, the dependence of the hyperpolarizabilities upon the geometry of the graph is reflected by the positions of the edges.

The sets of spectra and transition moments for an ensemble of quantum graphs with identical topology are used in the MC calculation to compute an ensemble of hyperpolarizability tensors. Each tensor is normalized to its extreme values as set by the theory of fundamental limits,[13] thus providing scale-independent results:

$$\beta_{max} = 3^{1/4}\left(\frac{e\hbar}{m^{1/2}}\right)^3 \frac{N^{3/2}}{E_{10}^{7/2}} \tag{4}$$

and

$$\gamma_{max} = 4\left(\frac{e^4\hbar^4}{m^2}\right)\frac{N^2}{E_{10}^5}. \tag{5}$$

Our work focuses on off-resonance phenomena so that the first and second hyperpolarizability tensors are fully symmetric in all indices and contain four and five independent components, respectively. Throughout this paper, all tensor components of the hyperpolarizabilities are normalized by these maxima, ie,

$$\gamma_{ijkl} \to \frac{\gamma_{ijkl}}{\gamma_{max}} \qquad \beta_{ijkl} \to \frac{\beta_{ijkl}}{\beta_{max}}. \tag{6}$$

The second hyperpolarizability normalized this way has a largest negative value equal to $-(1/4)$ of the maximum value. Normalized to their extreme values, the first intrinsic hyperpolarizability tensor for 2D graphs may then be written as

$$\beta_{ijk} \equiv \frac{\beta}{\beta_{max}} = \left(\frac{3}{4}\right)^{3/4} {\sum_{n,m}}' \frac{\xi_{0n}^i \bar{\xi}_{nm}^j \xi_{m0}^k}{e_n e_m}, \tag{7}$$

where ξ_{nm}^i and e_n are normalized transition moments and energies, defined by

$$\xi_{nm}^i = \frac{r_{nm}^i}{r_{01}^{max}}, \qquad e_n = \frac{E_{n0}}{E_{10}}, \tag{8}$$

with $r^{i=1} = x$ and $r^{i=2} = y$, and where

$$r_{01}^{max} = \left(\frac{\hbar^2}{2mE_{10}}\right)^{1/2}. \tag{9}$$

r_{01}^{max} represents the largest possible transition moment value of r_{01}. According to Eqn. (8), $e_0 = 0$ and $e_1 = 1$. β_{ijk} is scale-invariant and can be used to compare molecules of different shapes and sizes. Similarly, the second intrinsic hyperpolarizability tensor is given by

$$\gamma_{ijkl} = \frac{1}{4}\left(\sum_{n,m,l}{}' \frac{\xi_{0n}^i \bar{\xi}_{nm}^j \bar{\xi}_{ml}^k \xi_{l0}^l}{e_n e_m e_l} - \sum_{n,m}{}' \frac{\xi_{0n}^i \xi_{n0}^j \xi_{0m}^j \xi_{m0}^k}{e_n^2 e_m}\right). \tag{10}$$

The specification of a graph through its vertices, the calculation of its states and spectra, and the sampling of large numbers of geometries to create ensembles of transition moments, energies, and hyperpolarizabilities, is a Monte Carlo computation. The results of such a calculation are a set of tensors for a topological class of graphs whose variability is solely determined by the geometrical properties of the graphs. Using the rotation properties of the tensors, it is straightforward to identify the preferred diagonal orientation for any specified graph,[3] the one for which the hyperpolarizability along a specific axis is maximum. It is typical for β_{xxx} and γ_{xxxx} to be largest along different axes.[2]

A full contraction of all indices on either of the hyperpolarizability tensors creates an invariant under O(3) rotations called the tensor norm. Tensor norms provide insight into the limiting response of a specific graph topology for any of the realizable geometries. They are given by

$$|\beta| = \left(\beta_{xxx}^2 + 3\beta_{xxy}^2 + 3\beta_{xyy}^2 + \beta_{yyy}^2\right)^{1/2} \tag{11}$$

and

$$|\gamma| = \left(\gamma_{xxxx}^2 + 4\gamma_{xxxy}^2 + 6\gamma_{xxyy}^2 + 4\gamma_{xyyy} + \gamma_{yyyy}^2\right)^{1/2} \tag{12}$$

The use of tensors to extract the nonlinear optical response as a function of geometry and topology is most easily achieved by transforming the Cartesian tensors to spherical tensors. The transformation from a Cartesian to a spherical tensor representation is achieved using Clebsch-Gordon coefficients and has been extensively discussed in the literature,[14,15] as has their application.[3,16] The third rank symmetric Cartesian tensor β_{ijk} may be written as a sum of irreducible sets $J = 1$ and $J = 3$ of spherical tensors, while γ_{ijkl} decomposes into a set of irreducible spherical tensors transforming as $J = 0$, $J = 2$, and $J = 4$ representations of the angular momentum operators. Explicit forms are provided elsewhere.[3,14] The advantage to the designer of nonlinear molecular nanowires of a spherical tensor decomposition is that it provides information about how the graph behaves under rotations, ie, as a vector, an octupole, etc.

The computational scheme delineated in this section may be called the standard model of nonlinear optical quantum graphs. It is straightforward to devise Monte Carlo simulations for any graph of interest. Our early work focused on closed loops,[1] open loops, edges, and stars,[3] and complex combinations of elementary graphs, or motifs.[4] The next section reviews the results for the topological dependence of the hyperpolarizabilities and their universal scaling properties.

3. RESULTS

Figure 2 displays the maximum β_{xxx} and the range of γ_{xxxx} for closed loop, wire, and barbell topologies (lower left in the figure) and graphs comprised of star vertices on the right side of the graph. The effect of topology is profound, as every graph containing a star vertex has a first hyperpolarizability that is at least one half of the fundamental limit from Monte Carlo simulations and over 2/3 of the limit from potential optimization. The second hyperpolarizability has a much larger range, as well, and most significantly, graphs with stars can have large, positive γ_{xxxx}, whereas closed loops never have positive γ_{xxxx}. The main conclusion from these results is that structures exhibiting multiple pathways in space for electron motion will cause a much larger nonlinear interaction with light than those whose electron motion is confined to a closed pathway or a single channel.

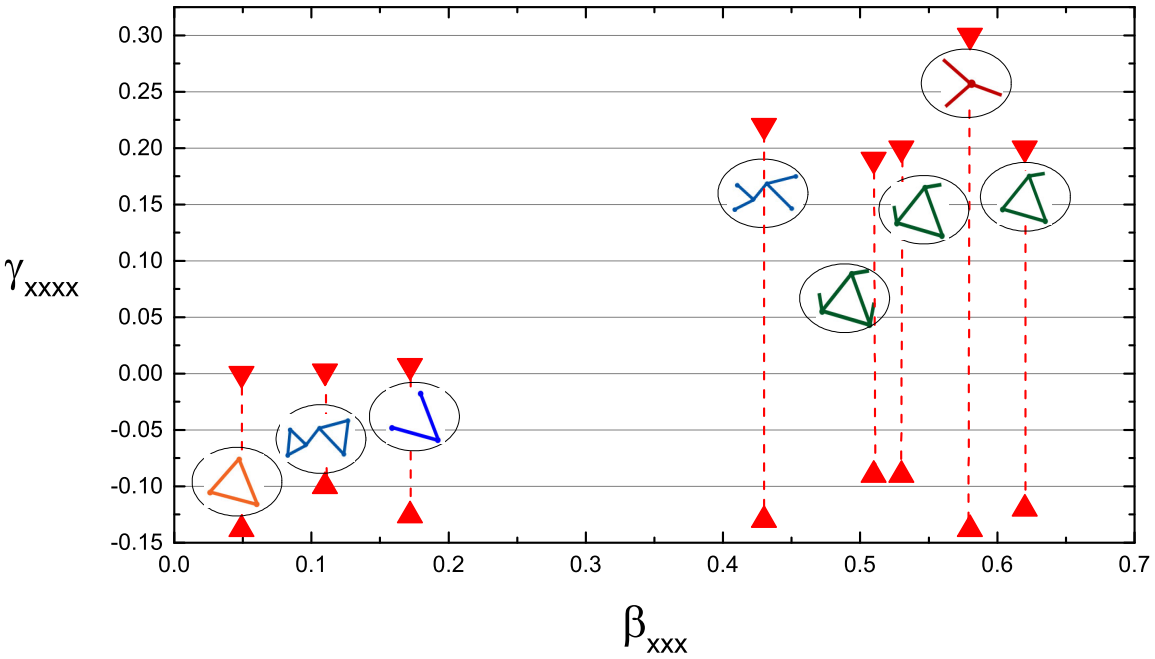

Figure 2. Topological dependence of β and γ. The dashed vertical lines show the range of γ_{xxxx}.

A closer, fundamental examination of the role of topology on nonlinear response may be obtained by appealing to the theory of fundamental limits,[13,17,18] in which the maximum values of β and γ are described in two basic model parameters related to the maximum transition moment and the ratio of the lowest energy differences. Empirically, the model seems applicable to systems near optimization and may in fact have universal properties for all graphs near their largest values.[19] Though Monte Carlo simulations based solely on sum rules produce the maximum values from this model,[20] studies which optimize the shape of the potential energy function[21–23] yield the largest possible nonlinear optical response of $\beta_{xxx} \simeq 0.71$ for a large set of potentials, which universally have the property that $X = x_{01}/x_{01}^{max} \simeq 0.79$ where x_{01}^{max} is given by

$$x_{01}^{max} = \left(\frac{\hbar^2}{2mE_{10}}\right)^{1/2}. \tag{13}$$

It is an empirical fact that systems near their optimum configuration get their contributions mainly from only three levels for β and at most four states for γ. In this three-level Ansatz, the normalized first hyperpolarizability β_{int} can be expressed as[24]

$$\beta_{int} = f(E)G(X), \tag{14}$$

where

$$f(E) = (1-E)^{3/2}\left(E^2 + \frac{3}{2}E + 1\right), \tag{15}$$

$$G(X) = \sqrt[4]{3}X\sqrt{\frac{3}{2}(1-X^4)}, \tag{16}$$

and $E = E_{10}/E_{20}$. Optimized systems will have β_{xxx} approaching $f(E)G(X)$, whereas systems far from optimum topology will show a gap between these values. Fig 3 provides a quantitative comparison of the potential optimization results for a closed loop topology (barbell) and the same geometry when the two bells are opened up (open barbell). This striking comparison reveals the impact of a change in topology on the scaling properties of the nonlinearities of the graphs.

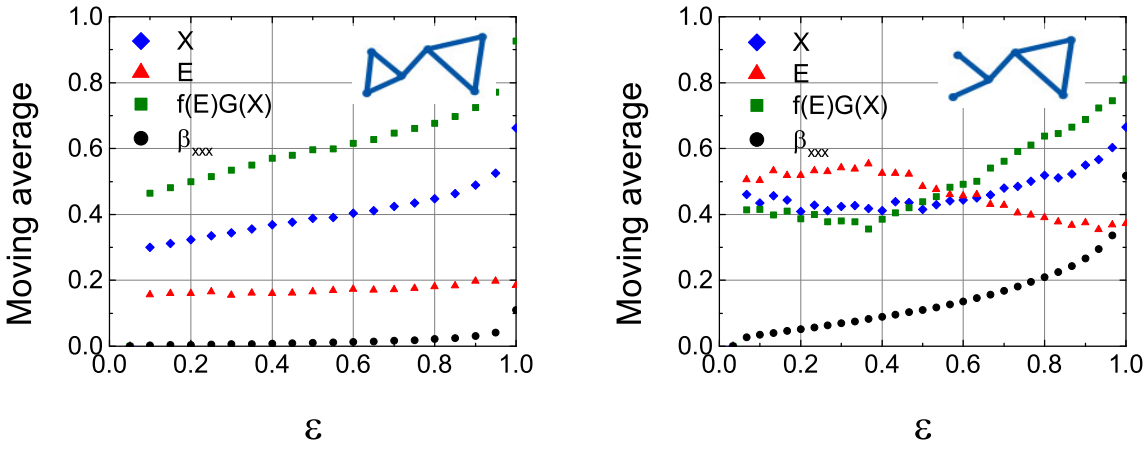

Figure 3. Scaling of three-level model parameters X, E, and fG for the closed (left) and open (right) barbell graphs. Here, ϵ is bin count, normalized to the total number of bins used in the moving average calculation.

4. CONCLUSIONS

We have reviewed our exact, quantitative analysis of the dependence of the nonlinear optics of quantum graphs on their geometry and topology. The effects of the topology of geometrically similar graphs dominate those of the geometry of topologically similar graphs. Topology largely determines the eigenstates and spectra, whereas the geometry mainly affects the projections of the graph edges onto the $x-y$ plane. Closed loop graphs always have non-optimum β and negative γ, but opening a vertex immediately raises β by over a factor of three and enables graphs with positive γ. Additional degrees of freedom enhance the nonlinearity of the graph, unless a fundamental topological constraint is in place.

ACKNOWLEDGMENTS

S. Shafei and M. G. Kuzyk would like to thank the National Science Foundation (NSF) (ECCS-1128076) for generously supporting this work.

REFERENCES

[1] S. Shafei, R. Lytel, and M. G. Kuzyk, "Geometry-controlled nonlinear optical response of quantum graphs," *J. Opt. Soc. Am. B* **29**, pp. 3419–3428, 2012.

[2] R. Lytel, S. Shafei, and M. G. Kuzyk, "Nonlinear optics of quantum graphs," in *Proc. SPIE 8474*, pp. 84740O–84740O–9, 2012.

[3] R. Lytel, S. Shafei, J. H. Smith, and M. G. Kuzyk, "Influence of geometry and topology of quantum graphs on their nonlinear optical properties," *Phys. Rev. A* **87**, p. 043824, Apr 2013.

[4] R. Lytel, S. Shafei, and M. G. Kuzyk, "Scaling and universality in nonlinear optical quantum graphs containing star motifs," *arXiv preprint arXiv:1305.4334* , 2013.

[5] S. Shafei and M. G. Kuzyk, "The effect of extreme confinement on the nonlinear-optical response of quantum wires," *J. Nonl. Opt. Phys. Mat.* **20**, pp. 427–441, 2011.

[6] T. Kottos and U. Smilansky, "Quantum chaos on graphs," *Phys. Rev. Lett.* **79**, pp. 4794–4797, Dec 1997.

[7] R. Blümel, Y. Dabaghian, and R. V. Jensen, "Explicitly solvable cases of one-dimensional quantum chaos," *Phys. Rev. Lett.* **88**, p. 044101, Jan 2002.

[8] R. Blümel, Y. Dabaghian, and R. V. Jensen, "Exact, convergent periodic-orbit expansions of individual energy eigenvalues of regular quantum graphs," *Phys. Rev. E* **65**, p. 046222, Apr 2002.

[9] Y. Dabaghian and R. Blümel, "Explicit spectral formulas for scaling quantum graphs," *Phys. Rev. E* **70**, p. 046206, Oct 2004.
[10] Y. Dabaghian and R. Blümel, "Explicit analytical solution for scaling quantum graphs," *Phys. Rev. E* **68**, p. 055201, Nov 2003.
[11] P. Kuchment, "Quantum graphs: I. some basic structures," *Wave Random Media* **14**(1), pp. 107–128, 2004.
[12] S. Shafei and M. G. Kuzyk, "Critical role of the energy spectrum in determining the nonlinear-optical response of a quantum system," *J. Opt. Soc. Am. B* **28**, pp. 882–891, 2011.
[13] M. G. Kuzyk, "Physical Limits on Electronic Nonlinear Molecular Susceptibilities," *Phys. Rev. Lett.* **85**, p. 1218, 2000.
[14] J. Jerphagnon, D. Chemla, and R. Bonneville, "The description of the physical properties of condensed matter using irreducible tensors," *Adv. Phys.* **27**(4), pp. 609–650, 1978.
[15] T. Bancewicz and Z. Ożgo, "Irreducible spherical representation of some fourth-rank tensors," *J. Comput. Meth. Sci. Eng.* **10**(3), pp. 129–138, 2010.
[16] M. Joffre, D. Yaron, J. Silbey, and J. Zyss, "Second Order Optical Nonlinearity in Octupolar Aromatic Systems," *J . Chem. Phys.* **97**(8), pp. 5607–5615, 1992.
[17] M. G. Kuzyk, "Fundamental limits on third-order molecular susceptibilities," *Opt. Lett.* **25**, p. 1183, 2000.
[18] M. G. Kuzyk, J. Perez-Moreno, and S. Shafei, "Sum rules and scaling in nonlinear optics," *Phys. Rep* **529**, pp. 297–398, 2013.
[19] S. Shafei and M. G. Kuzyk, "The paradox of the many-state catastrophe of fundamental limits and the three-state conjecture," *arXiv preprint arXiv:1306.0937* , 2013.
[20] M. C. Kuzyk and M. G. Kuzyk, "Monte Carlo Studies of the Fundamental Limits of the Intrinsic Hyperpolarizability," *J. Opt. Soc. Am. B.* **25**(1), pp. 103–110, 2008.
[21] J. Zhou, M. G. Kuzyk, and D. S. Watkins, "Pushing the hyperpolarizability to the limit," *Opt. Lett.* **31**, p. 2891, 2006.
[22] J. Zhou, U. B. Szafruga, D. S. Watkins, and M. G. Kuzyk, "Optimizing potential energy functions for maximal intrinsic hyperpolarizability," *Phys. Rev. A* **76**, p. 053831, 2007.
[23] T. Atherton, J. Lesnefsky, G. Wiggers, and R. Petschek, "Maximizing the hyperpolarizability poorly determines the potential," *J. Opt. Soc. Am. B* **29**, pp. 513–520, 2012.
[24] M. G. Kuzyk, "Using fundamental principles to understand and optimize nonlinear-optical materials," *J. Mat. Chem.* **19**, pp. 7444–7465, 2009.